Journal of *Marine Science and Engineering*

MDPI

Article

Sedimentary Characteristics and Model of Lacustrine Deep Water Gravity Flow in the Third Member of Paleogene Shahejie Formation in Niuzhuang Sag, Bohai Bay Basin, China

Yuanpei Zhang [1], Jun Xie [1,*], Kuiyan Gu [2], Haibo Zhao [3], Chuanhua Li [3] and Xiaofan Hao [1]

[1] College of Earth Science and Engineering, Shandong University of Science and Technology, Qingdao 266590, China; zhangyp0532@163.com (Y.Z.); haoxf0532@163.com (X.H.)
[2] Geophysical Research Institute of Shengli Oilfield, Sinopec, Dongying 257022, China; gukuiyan.slyt@sinopec.com
[3] Oil and Gas Exploration Management Center in Shengli Oilfield, Sinopec, Dongying 257000, China; zhaohaibo095.slyt@sinopec.com (H.Z.); lichuanhua.slyt@sinopec.com (C.L.)
* Correspondence: xiejun0532@163.com; Tel.: +86-137-0896-2993

Abstract: This article studies the sedimentary characteristics and models of the delta and gravity flow system of the third member of the Shahejie Formation in the Niuzhuang Sag area. Through seismic, logging, and core observation methods, a thorough investigation is conducted to examine the lithologic characteristics, grain size characteristics, sedimentary structure characteristics, and sedimentary facies distribution characteristics of this region. The results show that the third middle member of the Shahejie Formation in the Niuzhuang Sag can be classified into four sedimentary types: sliding, collapse, clastic flow, and turbidity flow. This article aimed to establish the distribution characteristics and depositional models of the deltaic and gravity flow depositional systems within the study area. The findings reveal that slip deposition primarily occurs near the delta front, while collapse and clastic flow depositions are concentrated near the far slope. Moreover, turbidity flow deposition is found near the far slope. This study significantly contributes to our understanding of the sedimentary characteristics and models associated with deltas and gravity flow systems in faulted lacustrine basins. Furthermore, it enriches existing theories related to gravity flow and provides a valuable reference for the investigation of deep-water sedimentation in continental faulted lacustrine basins.

Keywords: Bohai Bay Basin; Niuzhuang Sag; gravity flow; sedimentary characteristics; sedimentary model

check for updates

Citation: Zhang, Y.; Xie, J.; Gu, K.; Zhao, H.; Li, C.; Hao, X. Sedimentary Characteristics and Model of Lacustrine Deep Water Gravity Flow in the Third Member of Paleogene Shahejie Formation in Niuzhuang Sag, Bohai Bay Basin, China. *J. Mar. Sci. Eng.* **2023**, *11*, 1598. https://doi.org/10.3390/jmse11081598

Academic Editor: Dimitris Sakellariou

Received: 13 July 2023
Revised: 5 August 2023
Accepted: 13 August 2023
Published: 16 August 2023

Copyright: © 2023 by the authors. Licensee MDPI, Basel, Switzerland. This article is an open access article distributed under the terms and conditions of the Creative Commons Attribution (CC BY) license (https://creativecommons.org/licenses/by/4.0/).

1. Introduction

Deep-water (in which the general water depth is 1500~1800 m, the minimum depth is 100 m, and the maximum depth is 8000 m) gravity flow deposits have significant potential for oil and gas exploration. Deep-water gravity flows are crucial in transporting sediments from shallow-water environments to deeper waters. Therefore, studying deep-water gravity flow deposits in lacustrine environments is critical [1–3]. The theory of deep-water gravity flow deposits has advanced rapidly, and since the 1970s, gravity flow sedimentation theory has been extensively applied in numerous continental lacustrine basins in China, including the Songliao Basin [4], the Ordos Basin [5,6], the Bohai Bay Basin [7,8], and the Tarim Basin [9]. In recent years, the field of deep-water sedimentology has witnessed the emergence of new concepts and models [10,11], such as sandy clastic flows and muddy clastic flows, which are frequently used to explain the transport and deposition processes of deep-water blocky sandstones in continental lacustrine basins. In short, whether in the ocean or in lakes, gravity flow is a high-density underflow that flows along underwater slopes or canyons, contains a large amount of sand and mud, and is transported

in a suspended manner. That is to say, gravity flow is different from general flow. It is a high-density flow containing a large amount of mud, sand, gravel, and other detrital materials. These materials are transported in a suspended state, flowing under a water body with a lower density, and the flow rate is large. It is a non-Newtonian fluid. For instance, in the Yanchang Formation of the Ordos Basin, there has been a thorough investigation regarding the transition from sandy clastic flow to turbidity flow [12]; moreover, in the Jiyang depression of the Bohai Bay Basin, a detailed study has been conducted on the genesis of submarine gravity flows [13]. Additionally, the delta-fed gravity flow deposition model of the Dongying Depression of the Bohai Bay Basin has gained considerable attention [14]. Despite these advances, challenges still exist in deep-water oil and gas exploration, including low success rates in exploration and the unclear identification of areas with high-yield accumulations. These challenges stem from an inadequate understanding of the distribution patterns and characteristics of deep-water gravity flow sand bodies. Our understanding of the distribution of gravity flow sedimentary sand bodies and high-quality reservoirs is hindered by fundamental sedimentological issues, particularly in recent years with the development of new foundational theories pertaining to deep-water gravity flow sedimentation. These new theories provide a basis for re-evaluating several fundamental sedimentological issues in deep-water oil and gas exploration.

Recently, guided by new concepts and models in deep-water sedimentology, such as sandy clastic flows, blocky sandstone transport, and cohesive/weakly cohesive/non-cohesive clastic flows, several researchers have proposed novel perspectives on and insights into gravity flow systems [15–17]. However, the proliferation of various types and models of gravity flows has resulted in a lack of clarity in the terminology. This not only has perplexed subsequent researchers but also impeded comparative studies of distinct deep-water sedimentary units in different regions. The most notable debate centers around distinguishing high-density turbidity flow from sandy clastic flows [18,19]. Additionally, there is debate regarding whether deep-water sedimentary units with slumping structures should be encompassed within the scope of turbidites [20,21] due to their deviation from the typical characteristics of turbidite sedimentation. Simultaneously, differences also exist in the subdivision of sandy and muddy clastic flows [22,23], specifically in mudflow deposits (blocky mudstones containing floating gravel). Some argue that muddy clastic flows encompass mudflows [24], while others tend to differentiate mudflow deposits from muddy clastic flows and sandy clastic flows [7]. However, the discrepancy between mudflows and muddy clastic flows mainly lies in subtle variations in clay content, which proves challenging to discern in practice.

There are several types of gravity flow sedimentations, and classification schemes have progressed from rheology- or support mechanism-based classifications to the concept of sandy clastic flows based on rheology and sediment transport mechanisms. Based on their formation processes, they can be classified into four types: sliding, collapse, clastic flow, and turbidity flow [1]. This classification has gained wide acceptance among Chinese scholars and has been used for many applications [25–27]. Currently, research on the sedimentary characteristics of gravity flow deposits is relatively advanced. However, many exploration wells have limited core recovery, which makes it challenging to effectively reflect the spatial distribution of gravity flow sand bodies. Numerous studies have reported a close relationship between the sedimentary features and distribution patterns of deep-water gravity flows in continental lacustrine basins in China and large lake deltas [28,29]. Consequently, based on core observations, this study aims to describe the sedimentary characteristics of gravity flow sand bodies in the third member of the Shahejie Formation in the Niuzhuang Sag in the Bohai Bay Basin. Furthermore, lithological logging identification research is conducted to summarize the distribution patterns of gravity flow sand bodies, providing a more reliable foundation for sand body prediction. This research holds significant importance in guiding the exploration and development of gravity flow oil and gas reservoirs.

2. Geological Setting

The Bohai Bay Basin is an overlapping composite basin from the Mesozoic–Cenozoic era situated in the southeastern region of the Eurasian Plate. It is located at the convergence point of three significant tectonic domains: the Pacific, the Tethys, and the Paleo-Asian oceans [30]. The geological and tectonic characteristics of this area are highly intricate, encompassing diverse geological structures such as faults, folds, and sedimentation. Specifically, it is situated in the southeastern part of the Jiyang Depression (Figure 1a). The specific area of focus in this study is the Niuzhuang Sag, which is situated in the eastern part of the Dongying Depression within the Bohai Bay Basin in Eastern China. It spans approximately 40 km in the east–west direction and 15 km in the north–south direction, covering an approximate area of 600 km^2 (Figure 1b). The Niuzhuang Sag is surrounded by several major structural belts, including the Minfeng Sag, the Lijin Sag, the Chen Guanzhuang–Wangjiagang fault structure belt, and the Boxing Sag. These belts extend eastward to the Guanglinan Sag. The Niuzhuang Sag can be described as a diamond-shaped sedimentary unit with a distinct north–south boundary controlled by east–west faults (Figure 1c).

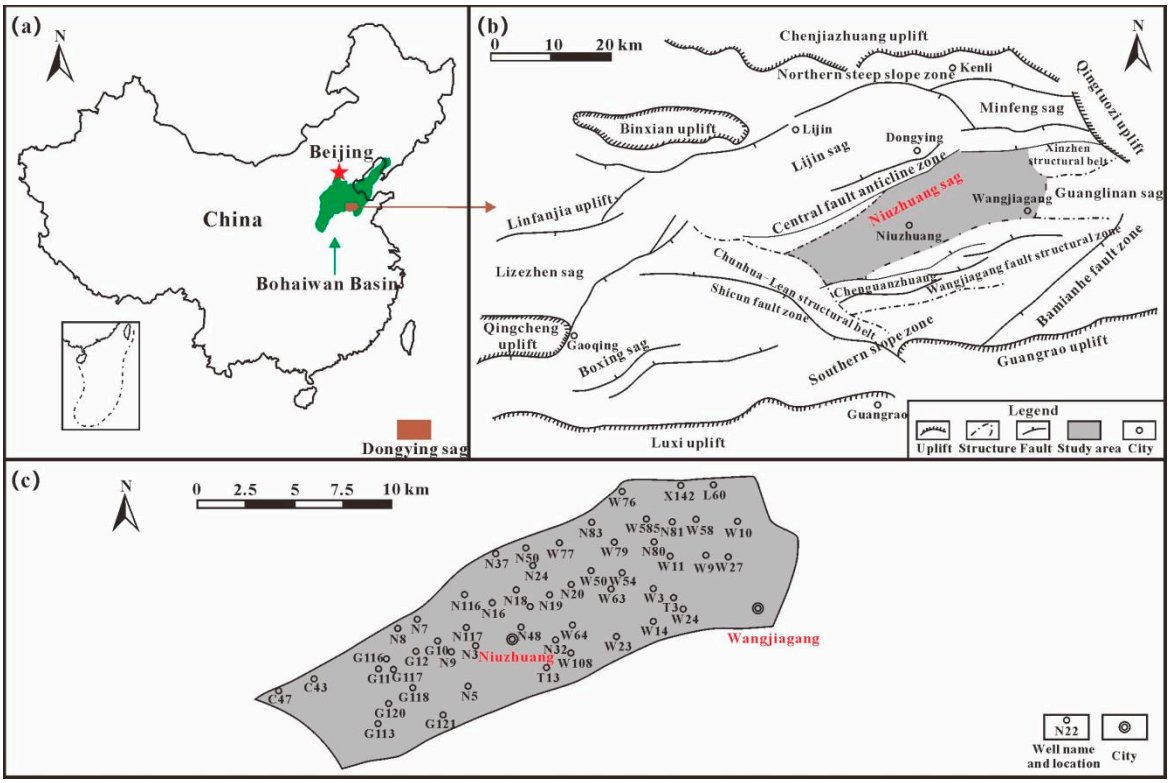

Figure 1. Location map of the study area. (**a**) Location of Bohai Bay Basin, (**b**) location of the study area, and (**c**) locations of wells in the study area.

The Paleogene stratigraphy of the Niuzhuang Sag comprises, from bottom to top, the Kongdian Formation (Ek), the Shahejie Formation (Es), and the Dongying Formation (Ed). Furthermore, the Neogene strata consist of the Guantao Formation (Ng) and Minghuazhen Formation (Nm) [31]. The target formation in this study is the third segment of the Shahejie Formation (Es_3), which is the thickest, most stable, and most significant reservoir of oil and gas in the area (Figure 2).

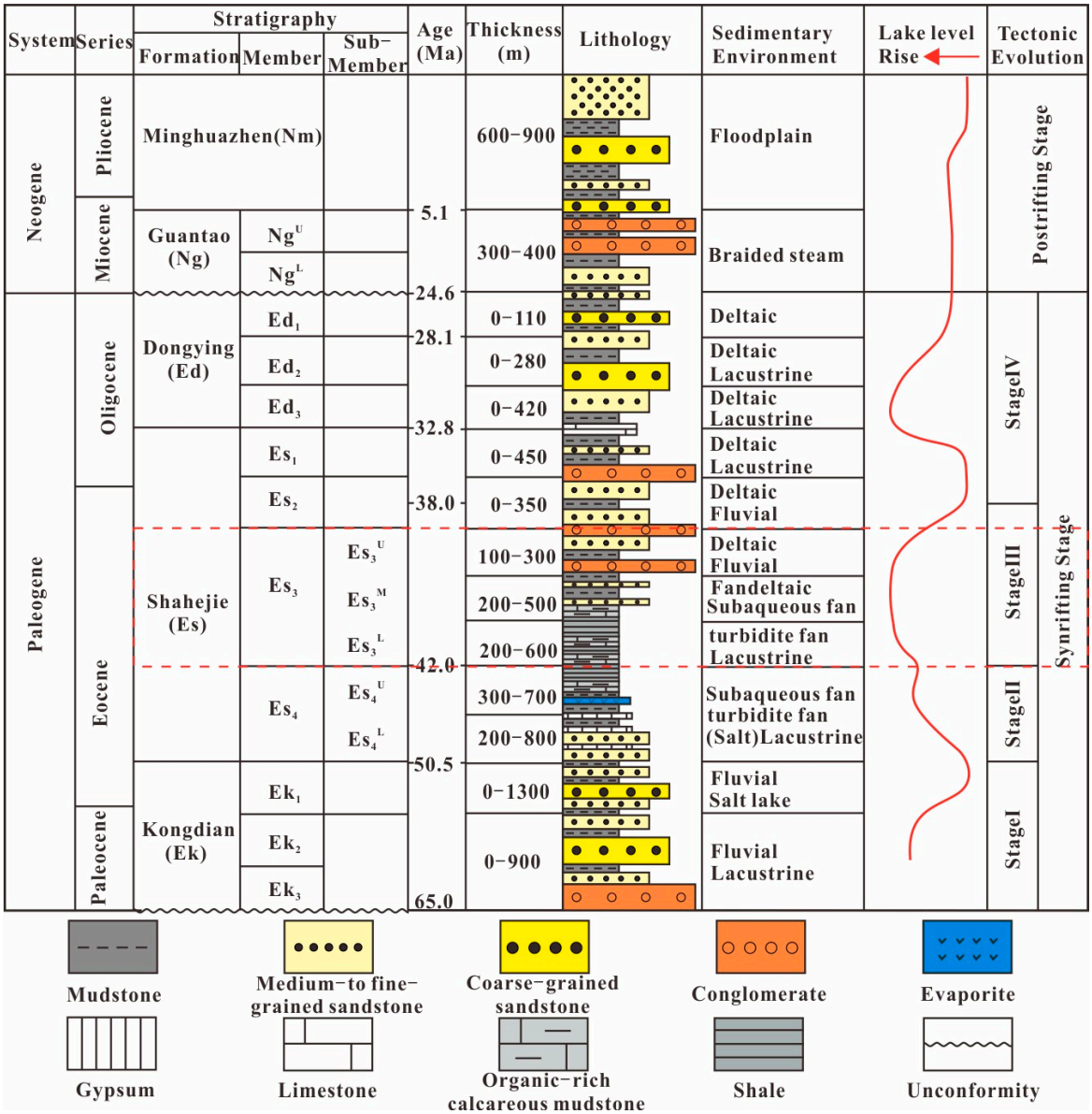

Figure 2. Comprehensive stratigraphic column of the Niuzhuang Sag [32].

3. Materials and Methods

3.1. Materials

Based on the observations and descriptions of 16 core wells in the Niuzhuang Sag, the third member of the Shahejie Formation (as shown in Table 1), along with the recent identification of gravity flow features in domestic and international studies, the sedimentary characteristics of gravity flow in various lithologies within the Niuzhuang Sag have been summarized. The predominant lithologies comprising gravity flow sediments include dark mudstone, sand–mud interbeds, siltstone, argillaceous siltstone, and fine sandstone, each exhibiting distinct sedimentary characteristics. Analysis of the gravity flow well core data indicates that the cored section corresponds to the third member of the Shahejie Formation, spanning depths ranging from 1960.00 m to 3405.60 m, with a total core length of 880.10 m.

Table 1. Coring data of gravity flow well.

Serial Number	Well Number	Top Depth/m	Bottom Depth/m	Horizon	Coring Length/m
1	G7	2078.15	2132.23	Es_3	51.6
2	G105	2149	2320.4		40.4
3	G112	2668.33	2693.83		25.2
4	N16	2973.37	3025.04		36.9
5	N21	2971	2966.5		103
6	N24	3055.34	3244.55		68.3
7	N30	2860	2865.75		46.5
8	N33	3028	3226		185
9	N43	3240	3378		42.3
10	N103	3056.04	3302.61		34
11	N104	2065.55	3117.3		57.7
12	N107	3026.8	3405.6		54.4
13	N301	2721	2792		31
14	W31	2445.07	2487.79		29.9
15	W35	1960	2015		52.7
16	W107	2600.5	2621.9		21.2

The primary classifications of sandstone encompass feldspathic sandstone and lithic feldspathic sandstone, characterized by a relatively low level of maturity regarding both their rock composition and structural development. The average quartz content is 44.5%, while the content of feldspar, which comprises potassium feldspar, plagioclase, and other variants, amounts to 15.4% (Table 2).

Table 2. Statistical table of clastic particle composition of Es_3 in the Niuzhuang Sag.

Well Number	Horizon/%	Quartz/%	Potassium Feldspar/%	Plagioclase/%	Mica/%	Matrix/%	Cement/%
N48	Es_3	40	10	27	1	1	4
N104		40	13	20	0.5	10	0
G10		48	14	14	0.5	10	0.5
N116		47	14	16	0.5	15	0.5
N117		55	18	14	0	10	0
G12		43	18	18	0.5	10	0
N107		42	16	15	2	10	5
N20		55	14	13	0	5	0
W108		36	18	14	0	2	0.5
N301		40	17	15	0.5	10	3
N33		45	10	10	0.5	7	1
W541		43	17	15	0.5	13	2

The rock stratigraphic assemblage of the third member of the Shahejie Formation in the study area consists of alternating layers of sand and mudstone. The clastic particles primarily exhibit secondary ribs with medium-good sorting, moderate weathering, porous cementation, and particle support. The dominant particle size ranges from 0.06 to 0.25 mm, indicating rapid deposition (Table 3). Overall, the sandstone in the study area exhibits a slightly poor to medium level of structural maturity and is close to the provenance.

Table 3. Statistics of structural maturity of some clastic rocks in Es_3.

Well Number	Horizon	Depth/m	Main Particle Size/mm	Sorting	Roundness	Support Mode	Cementation Type	Weathering Degree
N104	Es_3	3049.35	0.13–0.25	Good	Secondary edge	Particle	Pore	Medium
G10		2777.87	0.13–0.25	Medium				
N301		2721	0.06–0.13	Medium				
N301		2721	0.06–0.13	Poor-medium				
W541		2802	0.13–0.25	Medium				
N107		3269.1	0.13–0.25	Medium-good				
N301		2772	0.13–0.25	Medium-good				
W541		3049	0.13–0.50	Poor-medium				
W541		3073.64	0.13–0.25	Poor-medium				
W631		2768	0.13–0.25	Medium				
W631		2776.99	Unequal grain	Poor				
W631		2803.37	0.13–0.50	Medium				

3.2. Methods

This paper analyzes the delta and gravity flow system of the third member of the Shahejie Formation in the Niuzhuang Sag, Bohai Bay Basin. Our objective is to investigate the petrological characteristics, sedimentary structure characteristics, and logging facies characteristics of gravity flow fan bodies by analyzing and testing data, including core data and logging data. The sedimentary type of gravity flow is defined based on this analysis. Furthermore, the lithologic characteristics, grain size characteristics, and sedimentary structure of different types of gravity flow are thoroughly analyzed and summarized. Ultimately, the paper establishes the typical identification features of gravity flow sand bodies in different types within the delta front.

To achieve a fine core description and classify the sedimentary characteristics of gravity flow in the study area, a target well core from the Niuzhuang Sag with gravity flow development is selected. Physical sections and scan images of the core were utilized for this purpose. By combining the sedimentary characteristics and identification features of different gravity flow depositional types, the differences in gravity flow depositional types and vertical sequences across various distribution locations are clarified. This analysis is conducted by examining the gravity flow plane and profile phases, which allows for characterizing their distribution characteristics.

Rock samples were collected from 16 core wells at 30 different depths, and logging data were obtained from 60 wells. Microscopic characterization experiments, including thin slice analysis, scanning electron microscope analysis, and X-ray diffraction analysis, were conducted on these rock samples using optical or electron microscopy. A comprehensive analysis of particle size data from major core wells was also performed. Combined with other particle size parameter data, the particle size data were used to construct a probability accumulation curve. The CM value was obtained from this curve, and a CM graph was drawn. The 3D seismic data in the study area are provided by Sinopec Shengli Oil Field Exploration and Development Research Institute. The sampling rate is 4 ms, the amplitude range is −13,000~13,000, and the time depth of the target horizon is 2000~2600 ms. The main frequency of the target layer is 25 Hz, with a frequency band width of 10–60 Hz. The time axis of the main layers on the seismic profile is stable, with obvious faults. The average longitudinal wave velocity of the formation is 3500 m/s, and the seismic resolution is estimated to be 35 m. Based on seismic stratigraphy theory, Petrel software is used to interpret these data. Based on these findings, a systematic study was conducted regarding the core characteristics, sedimentary structure characteristics, delta depositional system distribution characteristics, and gravity flow characteristics of the third member of the Shahejie Formation in the Niuzhuang Sag. By examining the sedimentary characteristics, distribution, and internal structure of different gravity flow sand bodies in the study area, this paper establishes deltaic and gravity flow sedimentary models specific to the study area.

4. Sedimentary Characteristics

4.1. Lithologic Characteristics

The lithology of the third member of the Shahejie Formation in the Niuzhuang Sag primarily consists of fine siltstone and mudstone. The siltstone content reaches as high as 35.7%, and the mudstone accounts for 24.6%. Furthermore, fine sandstone comprises 24.2% of the formation, and pebbled sandstone represents 15.5% (Figure 3a). The predominant sandstone types observed are feldspar lithic sandstone and lithic feldspar sandstone, indicating low rock composition and structural maturity. The average quartz content amounts to 44.5%, while the feldspar content, which includes potassium feldspar and plagioclase, is 15.4% (Figure 3b).

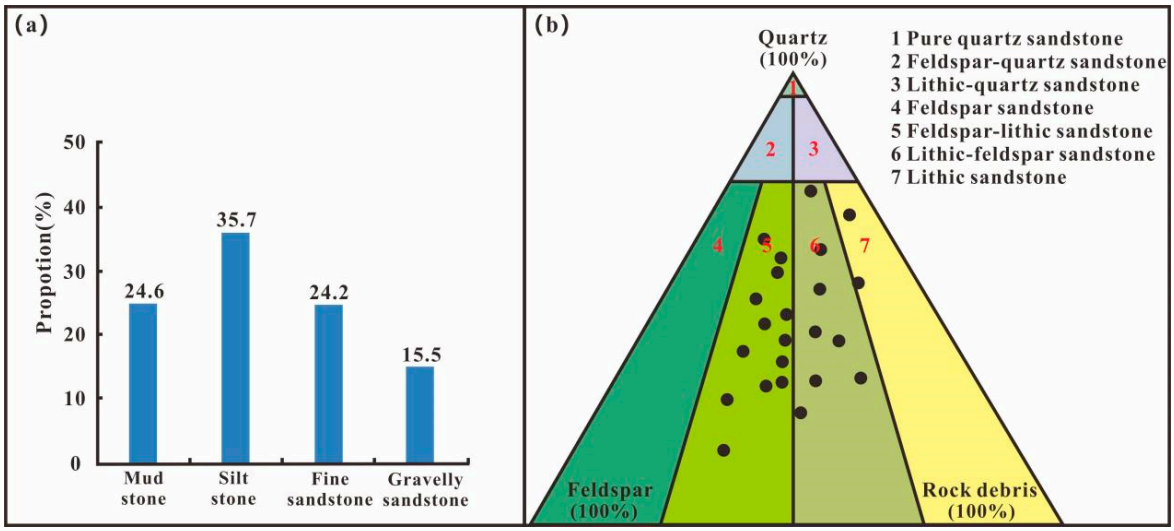

Figure 3. Rock types and major compositions. (**a**) Lithologic histogram and (**b**) sandstone type map.

4.2. Grain Size Characteristics

The cumulative probability curve of the delta front exhibits a three-stage distribution, as depicted in Figure 4a. This distribution indicates a significant slope in jump times (0.1 mm < particle size < 1 mm), suggesting a strong hydrodynamic force and a well-developed sorting effect on the sand bodies. In the CM diagram, the OP/PQ segment predominantly represents the traction flow in this region (Figure 4f). The cumulative curve for the probability of sliding, collapsing, and debris flow in the grain size of the sand bodies also demonstrates a three-stage or two-stage distribution. When the overall slope of the jump order is smaller than that of the delta front, there is an increase in the overall content of the suspension order. Consequently, the span of the grain size interval becomes larger, leading to a deterioration in the sorting effect (Figure 4b–d). In the CM diagram, the presence of OP (rolling-based) and PQ (suspension-based) segments indicates traction flow, while there is a significant increase in QR (progressive suspension) segments representing gravity flow (Figure 4f). Generally, both traction flow and gravity flow exhibit characteristic grain size behaviors. The probability accumulation curve of turbidity flow mainly displays a wide/slow upward arch or a single section (Figure 4e). In the CM diagram, turbidite types dominated by QR are observed (Figure 4f). This pattern reflects a typical graded suspended deposition in which the C value increases proportionally to the M value, resulting in a figure parallel to the C = M baseline.

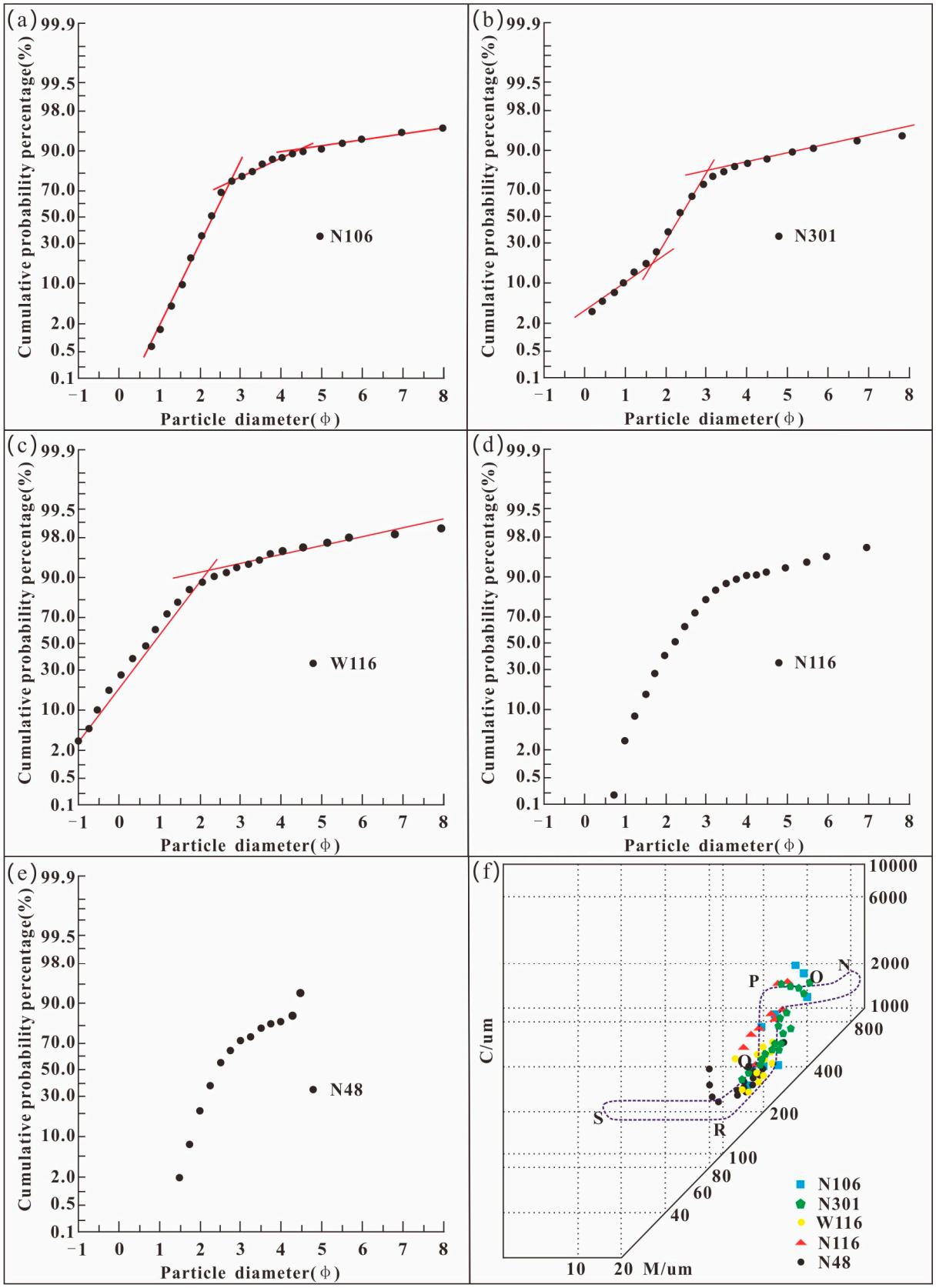

Figure 4. Grain size probability cumulative curve and CM diagram of sandstone. (**a**) N106 well probability cumulative curve; (**b**) N301 well probability cumulative curve; (**c**) W116 well probability cumulative curve; (**d**) N116 well probability cumulative curve; (**e**) N48 well probability cumulative curve; and (**f**) CM diagram.

4.3. Delta Sedimentary Characteristics

Based on the observation and analysis of seismic data, well logging information, and core characteristics, it is determined that the delta sand bodies in the Niuzhuang Sag primarily correspond to the delta front subfacies, which encompass two distinct types: underwater distributary channels and estuary bar sand bodies. The sand body of the underwater distributary channel exhibits a positive grain sequence (Figure 5a) and consists of medium-fine sandstone and argillaceous siltstone with massive bedding (Figure 5b) and scour and filling structures, reflecting the remote provenology and long-distance transport-based deposition. Conversely, the estuarine bar sand body exhibits a reverse grain sequence (Figure 5c) and is composed of sandy pure, well-sorted fine sandstone and siltstone. In addition, it exhibits wavy crossbedding (Figure 5d), tabular crossbedding (Figure 5e), and wavy sand-grained bedding (Figure 5f), reflecting the effects of wave erosion and the transformation of lake water.

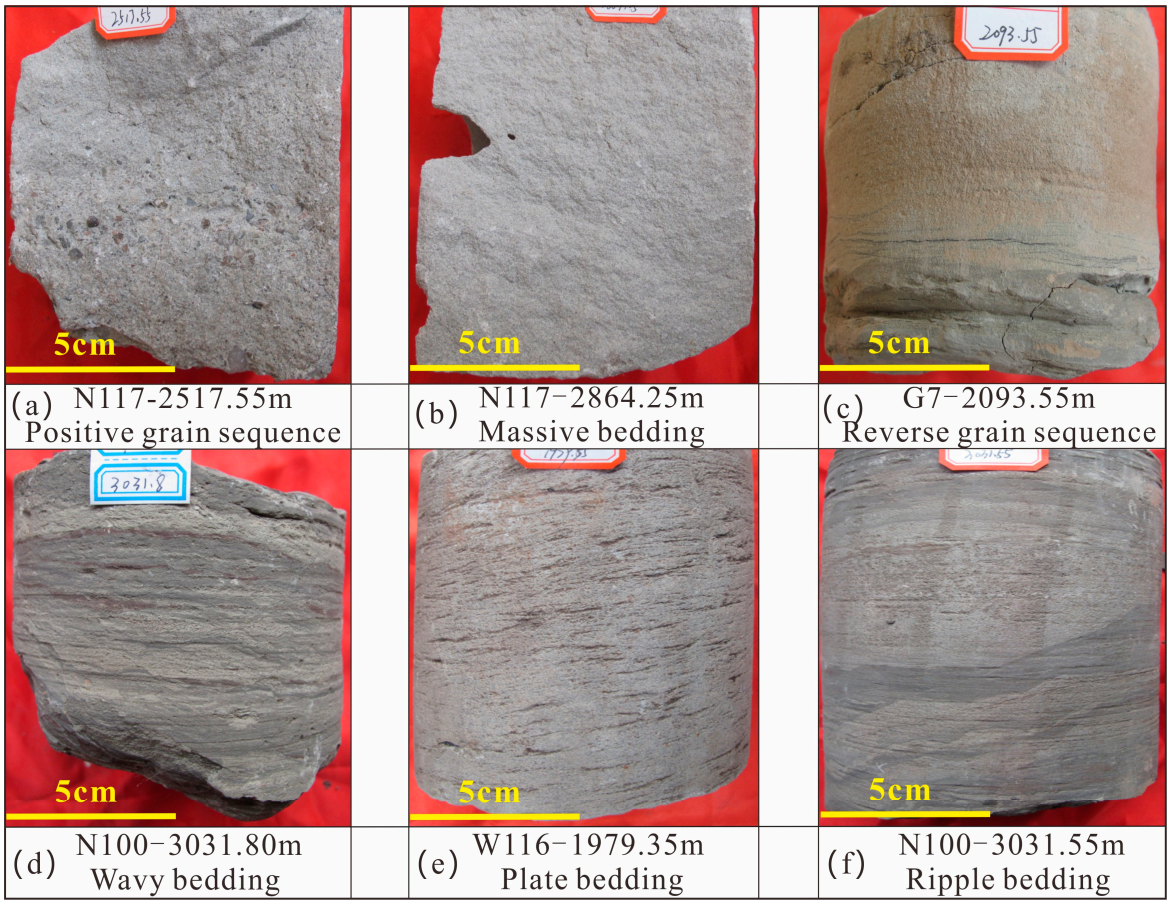

Figure 5. Sedimentary structure of delta front in the Niuzhuang Sag. (**a**) N117: 2517.55 m, positive grain sequence characteristics; (**b**) N117: 2864.25 m, massive medium sandstone; (**c**) G7: 2093.55 m, reverse grain sequence characteristics; (**d**) N100: 3031.80 m, wavy crossbedding; (**e**) W116: 1979.35 m, plate crossbedding; and (**f**) N100: 3031.55 m, wavy ripple bedding.

4.4. Sedimentary Characteristics of Gravity Flow

In the deep-water environment of the third member of the Shahejie Formation in the Niuzhuang Sag, the sand bodies of the delta front undergo sliding and collapsing, forming gravity flow deposits. By investigating the drilling cores, logging, and logging characteristics, the gravity flow sand bodies can be classified into four genetic types: sliding deposits, collapse deposits, clastic flow deposits, and turbidite deposits. These genetic types represent typical processes involved in delta formation and destruction.

4.4.1. Sliding Sedimentary Structure

Sliding deposition is a distinct sedimentary process typically occurring in regions experiencing significant geological activity, including earthquakes, volcanic eruptions, tsunamis, and waves. Under the influence of these conditions, blocks of sediment slide along shear planes, resulting in the formation of bulk flow deposits [33]. Due to the mechanical properties of elastic deformation, sliding deposition generally preserves the original sedimentary structure prior to sliding; however, the shear forces at the base cause deformation in the partially consolidated underlying sediments. In the Niuzhuang Sag, the sliding deposits exhibit deep-water dark mudstone at both the top and bottom, with the lithology predominantly composed of gray or gray siltstone and fine sandstone. Upon examination of the core samples, distinct features associated with sliding deposition are observed, including sliding planes (Figure 6a,b), sliding deformations (Figure 6c–e), and underlying sediment fold deformations (Figure 6f). Furthermore, certain sliding deposits exhibit shallow-water sedimentary structures, such as crossbedding and wavy bedding.

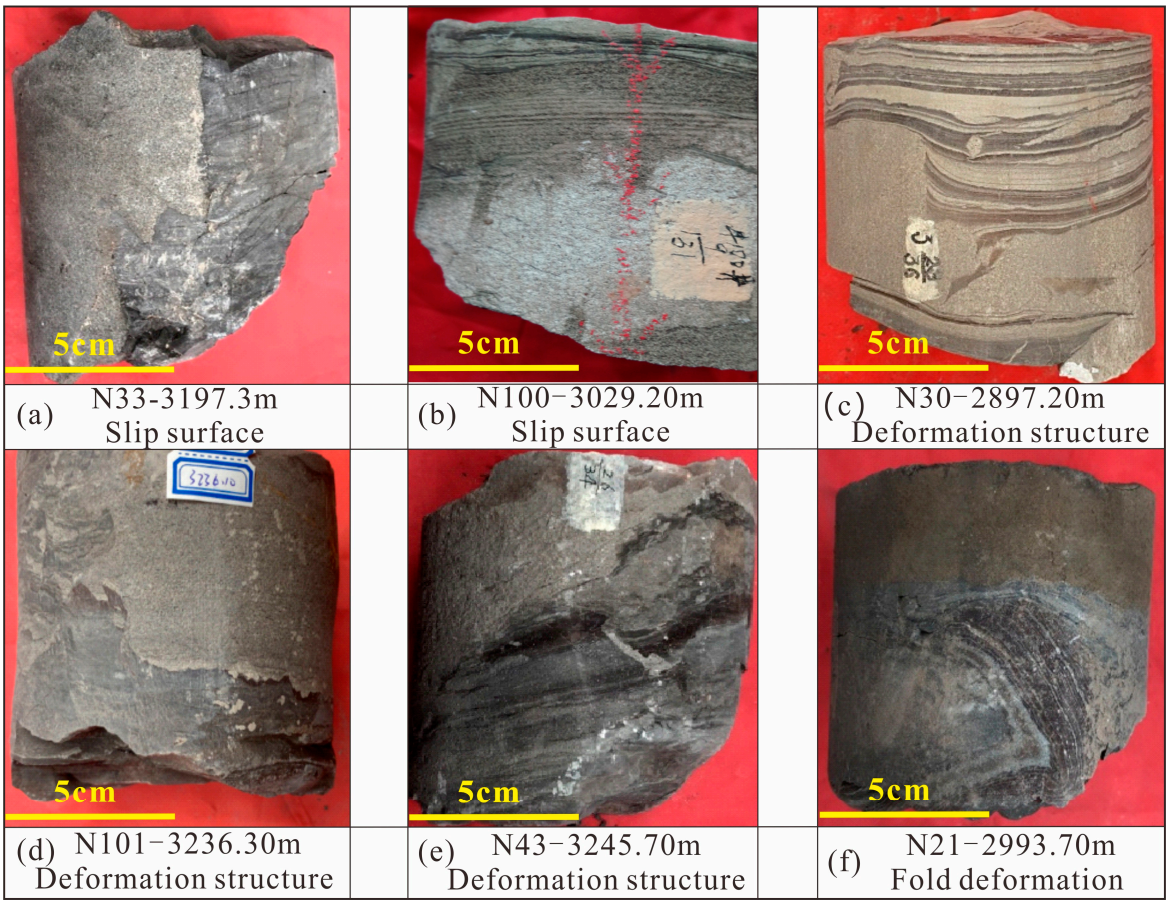

Figure 6. Sliding sedimentary structure in the Niuzhuang Sag. (**a**) N33: 3197.30 m, massive fine sandstone and internal high-angle secondary slip surface; (**b**) N100: 3029.20 m, sand injection bodies observed on the synsedimentary sliding surface; (**c**) N30: 2897.20 m, vein bedding, sliding, and deformation structure; (**d**) N101: 3236.30 m, sliding deformation structure; (**e**) N43: 3245.70 m, sliding deformation structure; and (**f**) N21: 2993.70 m, the sliding of the overlying sand body leading to the folding deformation of the underlying sand body.

4.4.2. Collapse Sedimentary Structure

Collapse deposition occurs when layers of sediment move along a sliding surface of a slope and undergo rotation due to the combined effects of gravity and shear forces [34]. The collapse deposits within the Niuzhuang Sag region primarily consist of gray and argillaceous siltstone. These rocks commonly exhibit various deformation structures,

including coiled bedding (Figure 7a), deformable structures (Figure 7b–d), flame-like structures (Figure 7e), and sandstone veins (Figure 7f). These characteristics serve as indicators of significant geological movement and deformation within the area, making them highly valuable for studying geological evolution history and conducting resource exploration.

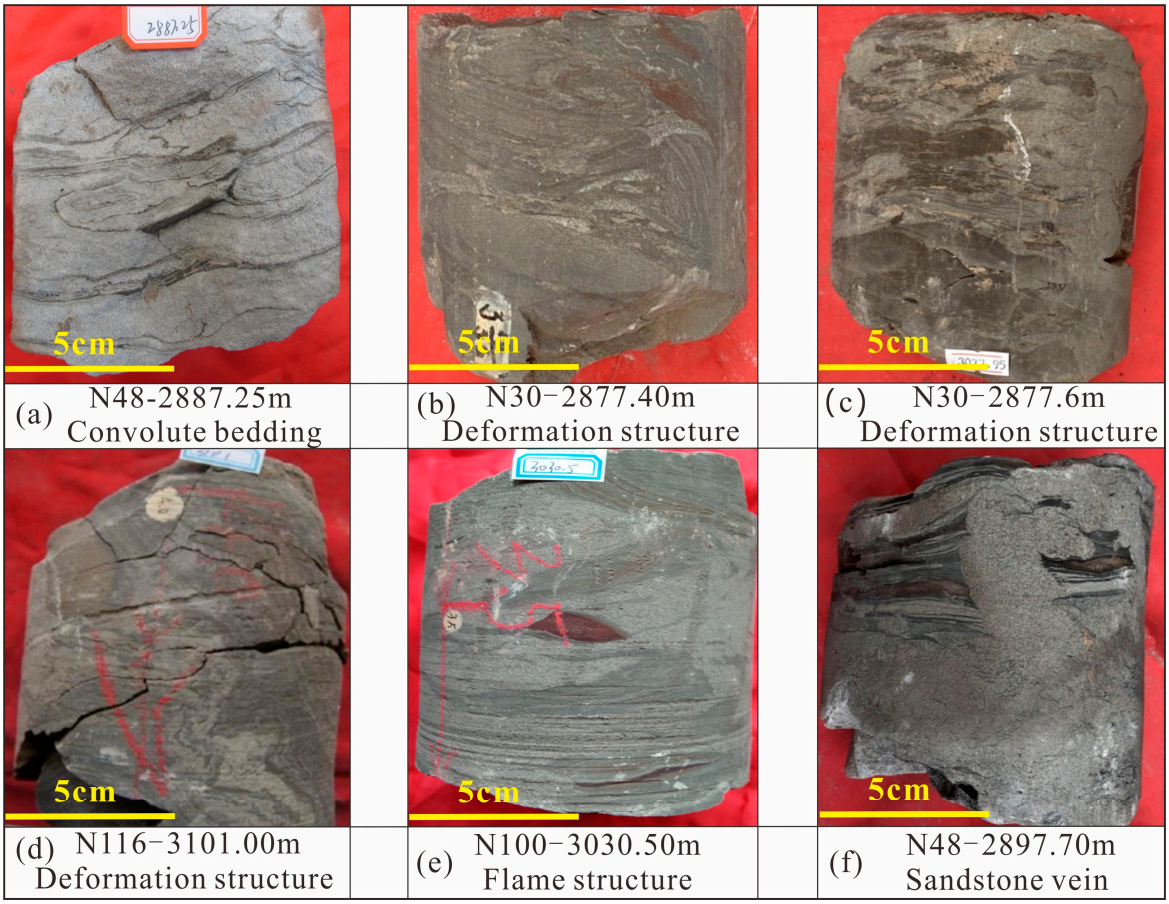

Figure 7. Collapse sedimentary structure of the Niuzhuang Sag. (**a**) N48: 2887.25 m, convolute bedding; (**b**) N30: 2877.40 m, collapse deformation structure; (**c**) N30: 2877.60 m, collapse deformation structure and sandstone veins filling upwards; (**d**) N116: 3101.00 m, collapse deformation structure; (**e**) N100: 3030.50 m, flame structure; and (**f**) N48: 2897.70 m, intestinal sandstone vein.

4.4.3. Clastic Flow Sedimentary Structure

Clastic flow is a non-Newtonian fluid exhibiting plastic behavior. It commonly undergoes deposition in a monolithic "frozen" manner, forming sandy clastic flow deposits [18,35]. Within the third member of the Shahejie Formation in the Niuzhuang Sag, clastic flow deposits of a significant scale exist. These deposits primarily consist of extensive medium-to-fine-grained sandstone, fine sandstone, and siltstone, associated with dark or brown mudstone. Clastic flow can be divided into two types: sandy debris flow and muddy debris flow. The core samples exhibit numerous fragments of torn mudstone debris (Figure 8a–c), and floating mudstones are frequently observed atop the sandstone layers (Figure 8d,e). Furthermore, planar clastic structures are prevalent (Figure 8f), often presenting sudden variations in contact with the underlying surface.

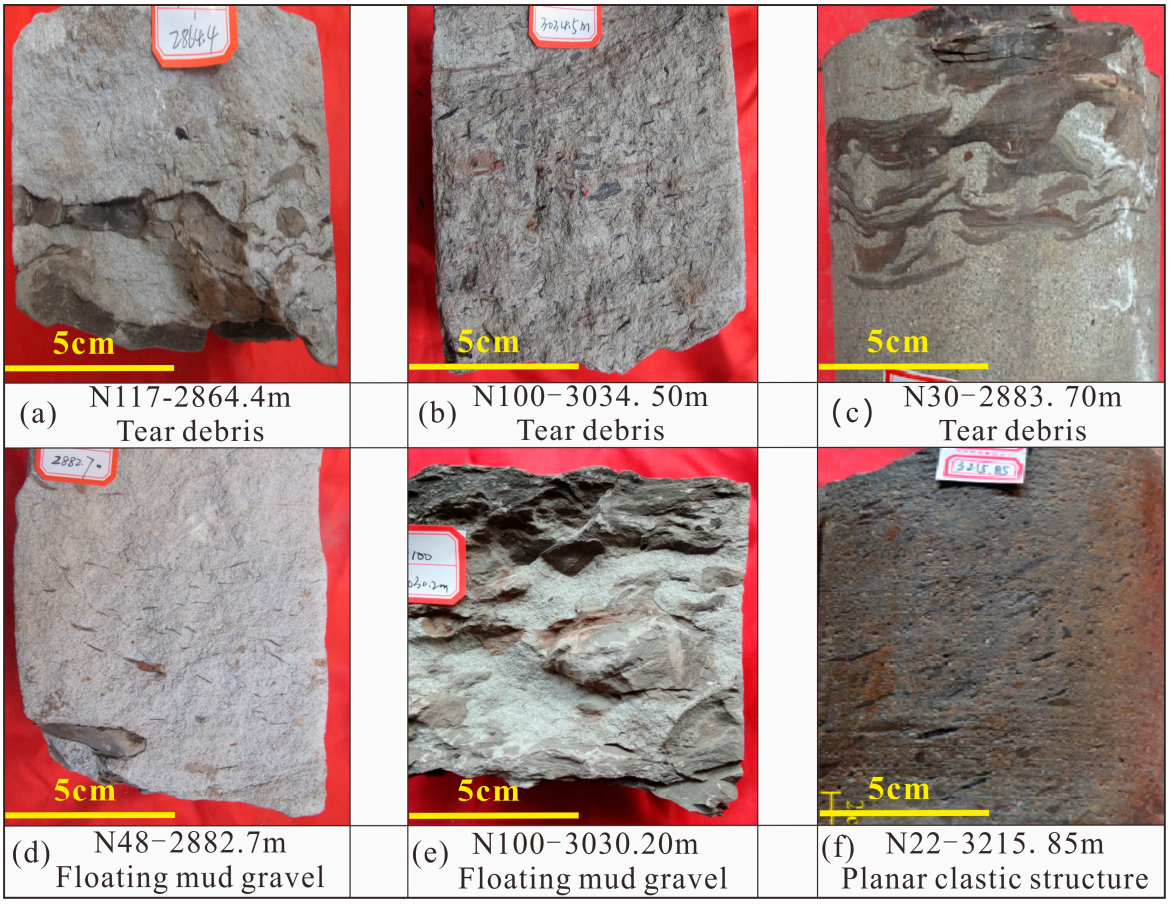

Figure 8. Clastic flow sedimentary structure of the Niuzhuang Sag. (**a**) N117: 2864.40 m, mudstone tear debris; (**b**) N100: 3034.50 m, a large amount of mudstone tear debris; (**c**) N30: 2883.70 m, the top of sandstone contains a large amount of mudstone tear debris; (**d**) N48: 2882.70 m, floating mud gravel in massive sandstone, and the long axis of mud gravel is parallel to the layer; (**e**) N100: 3030.20 m, massive sandstone contains a large amount of mud gravel; and (**f**) N22: 3215.85 m, massive sandstone with planar clastic structure, and the long axis of mud gravel is parallel to the bedding plane.

4.4.4. Turbidity Flow Sedimentary Structure

Turbidity flows are influenced by gravity and fluid dynamics. They typically contain a mixture of materials, including sand, mud, debris, and other sediments, which are transported and deposited by the motion of the fluids, forming irregular sedimentary structures [36]. The turbidity flows exhibit turbulent behavior, characterized by high energy and velocity, allowing them to transport and deposit sediment over long distances [37,38]. Turbidite deposits are primarily composed of thin layers of gray and argillaceous siltstone. These sediments are typically formed under relatively weak hydraulic conditions and possess a relatively low particle density. The turbidity flow deposits found in the third member of the Shahejie Formation in the Niuzhuang Sag have resulted due to low-density turbidity flows, indicating the prevailing weak hydrodynamic conditions in this area. In the core of the study area, distinct turbidite sedimentary features can be observed, such as the Bouma sequence (Figure 9a–d) and sand–mud interbeds (Figure 9e,f), which collectively form multiple sedimentary cycles.

The Bouma sequence is one of the important indicators for identifying turbidite deposits. It consists of five segments as follows, from bottom to top: A—the bottom progressive segment, B—the lower parallel lamina segment, C—the flowing water ripple segment, D—the upper parallel lamina segment, and E—the deep cement rock segment. The thickness of the Bouma sedimentary sequence formed by a turbidity current varies

greatly, ranging from several centimeters to several meters. Due to the influence of the frequency and intensity of the turbidity current and the erosion and scouring of the turbidity current again, the perfection of the Bouma sequence of Turbidite is destroyed, resulting in the formation of multiple sequences that lack certain intervals, such as ABCDE, BCDE, CDE, DE and AB, BC, CD, and other sequences.

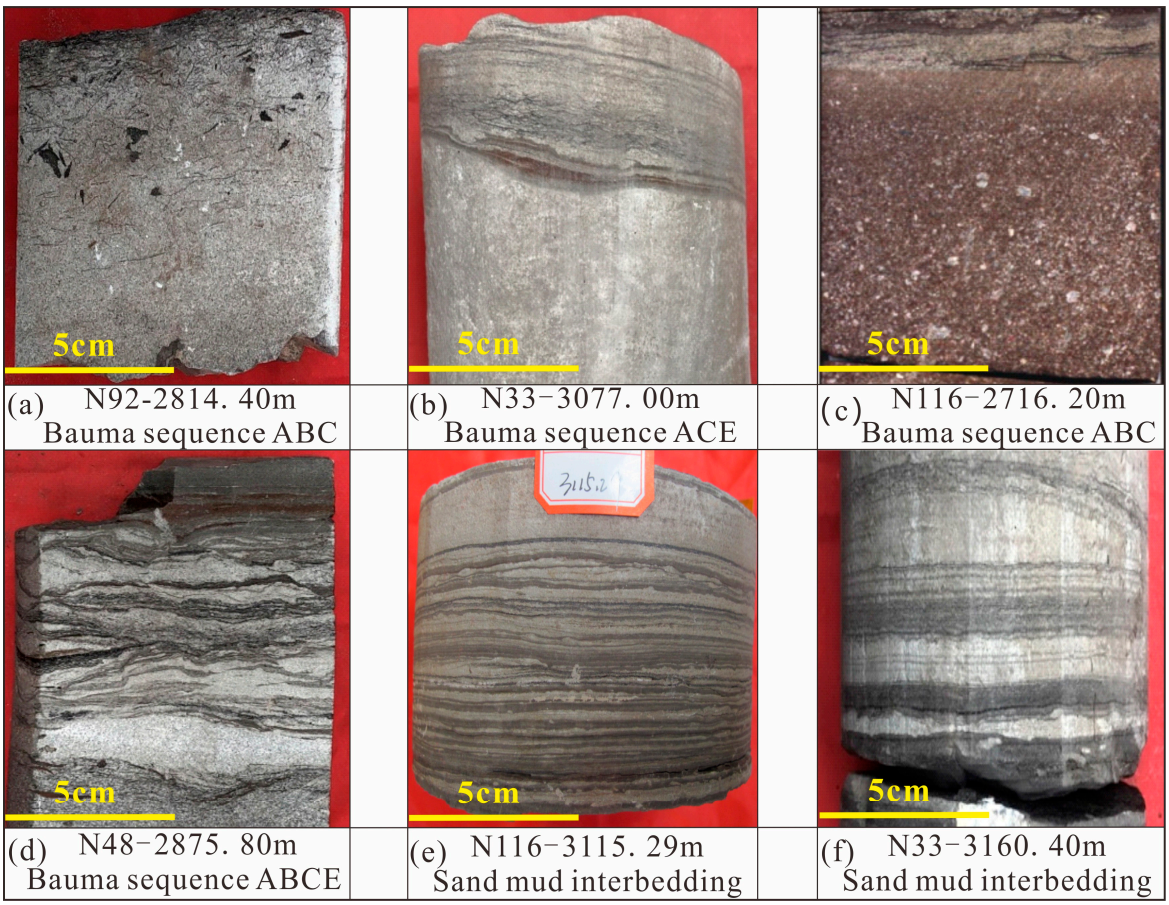

Figure 9. Turbidite flow sedimentary structure in the Niuzhuang Sag. (**a**) N92: 2814.40 m, Bouma sequence ABC; (**b**) N33: 3077.00 m, Bouma sequence ACE; (**c**) N116: 2716.20 m, Bouma sequence ABC; (**d**) N48: 2875.80 m, Bouma sequence ABCE; (**e**) N116: 3115.10 mm, sand–mud thin interbedding, forming multiple cycles; and (**f**) N33-3160.40 m, sand–mud interbedding, multiple sedimentary cycles.

4.5. Logging Facies Characteristics

Logging facies is a commonly employed technique for characterizing formation properties and distinguishing between different formations [39]. It is widely acknowledged that distinct formations can be distinguished by a set of logging response characteristics. The interpretation of sedimentary facies often involves the utilization of natural potential curves and natural gamma curves.

Within the study area's target interval, approximately five types of spontaneous potential logging curves can be identified (Figure 10). The sand bodies in underwater distributary channels exhibit positive grain sequences, manifesting as bell-shaped and box-shaped features on the spontaneous potential curve. However, the estuarine bar sand body exhibit a reversed grain sequence, leading to a funnel-shaped pattern on the natural potential curve. Deep-water sliding deposits are characterized by dark mudstone at the top and bottom, and the natural potential curves exhibit finger-shaped and funnel-shaped patterns with intermediate to high amplitudes. As indicated by their spontaneous potential curves, collapse deposits demonstrate a toothed bell-shaped pattern with intermediate to high

amplitudes. Furthermore, clastic flow deposition is identified by spontaneous potential curves displaying box-shaped and toothed patterns with intermediate to high amplitudes, occasionally exhibiting bell-shaped features as well. Turbidity flow deposition is associated with low finger-shaped and tooth-shaped patterns observed on the spontaneous potential curve.

Sedimentary type	SP	GR	Logging facies characteristics
Underwater distributary channel	N301 	N301 	Bell shape and box shape
Mouth bar	XX178 	XX178 	Funnel shape
Slide	N117 	N117 	Medium and high finger shape and funnel shape
Collapse	S10 	S10 	Medium and high amplitude toothed bell shape
Clastic flow	N30 	N30 	Medium and high amplitude toothed box shape and tooth shape
Turbidity current	N22 	N22 	Low amplitude finger and tooth shape

Figure 10. Logging facies characteristics in the Niuzhuang Sag.

4.6. Seismic Facies Characteristics

Seismic facies markers are prominent and easily identifiable markers within specific facies that can be utilized to identify geological formations [40,41]. The delta front sand bodies exhibit multiangle crossbedding, a medium to high amplitude, and a low frequency on the seismic facies, displaying characteristics of lens-shaped reflection structures. The seismic facies characteristics of gravity flow sand bodies can be categorized into four types. Sand bodies caused by sliding exhibit large shuttle-shaped reflections, a medium to strong amplitude, a low frequency, and moderate to low continuity. Sand bodies resulting from collapse exhibit prograding reflections at the forefront, complex wave patterns, a medium to strong amplitude, a medium frequency, and good continuity. Clastic-flow-induced sand bodies present parallel to near-parallel reflections, a weak to medium amplitude, a low frequency, and poor continuity. Finally, turbidites demonstrate small-sized overlapping

reflection structures, with a "wedge-shaped" bottom external reflection form and a low amplitude to medium-frequency discontinuous reflection signals. On the seismic profile, the gravity flow sand bodies within the study area are situated within the progradation layer, forming hills and wedge shapes, exhibiting chaotic reflection structures, disconnected from the front sand bodies, and laterally pinched out (Figure 11).

Sedimentary type	Seismic form	Core photo	Well & MD	Seismic facies characteristics
Delta front	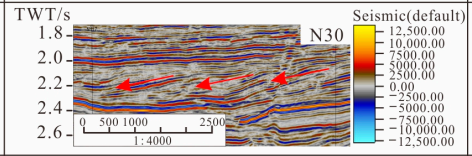		N30 2870.75m	Oblique progradation
Sliding sand body	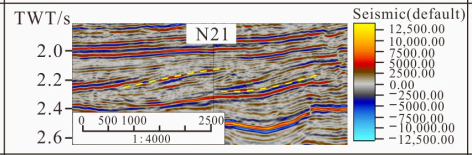		N21 2993.70m	The external reflection structure is large shuttle reflection
Collapse sand body	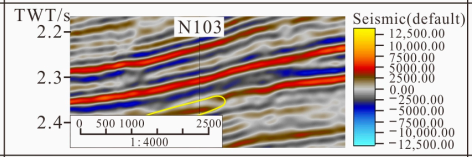		N103 3123.20m	Leading edge of progradation reflection
Clastic flow sand body	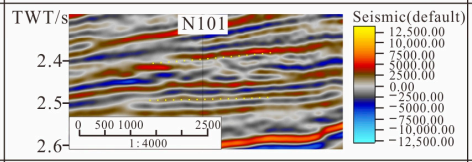		N101 3216.90m	Parallel near parallel reflection
Turbidite sand body	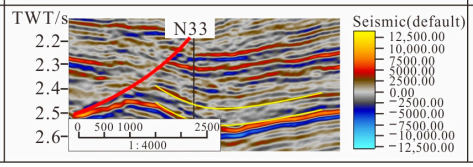		N33 3460.40m	Small overlapping reflection structure, and the external reflection shape at the bottom is similar to "wedge"

Figure 11. Seismic facies characteristics in the Niuzhuang Sag.

5. Discussion

5.1. Profile Distribution Characteristics of Sedimentary Microfacies

During the deposition period of the third member of the Shahejie Formation, a delta front developed in the study area, primarily concentrated in the southeast region, following the direction of the provenance supply. Furthermore, the delta front extended below the lake shoreline. Over time, the depression in the lake basin before the delta front experienced resedimentation, leading to slip and slump deposits. With continuous deposition, the delta deposition gradually filled the Niuzhuang Sag and expanded toward the center of the lake basin. The significant influence of deltaic progradation caused the continuous sedimentation of the deltaic plain and front sediments toward the center of the lake basin, resulting in a progressive filling trend. Simultaneously, this process induced the gradual migration of the marginal slope toward the center of the lake basin while pushing the development of gravity flow deposition along the provenance supply direction to the same central area (Figure 12).

5.2. Plane Distribution Characteristics of Sedimentary Microfacies

Based on the planar distribution characteristics of sand bodies and sedimentary microfacies, the delta in the Niuzhuang Sag underwent progradation from the southeast to the northwest during the third member of the Shahejie Formation. Therefore, the delta primarily comprises two types of sand bodies: underwater distributary channels and estuary bars. Concurrently, a series of gravity flow sand bodies with different origins,

including sliding, collapse, clastic flow, and turbidity flow deposits, formed within the shore-shallow lake and semi-deep/deep-lake lake subphases. In the horizontal plane, the sliding deposits are situated closest to the delta front, exhibiting a zonal pattern that runs parallel to the sand bodies along the delta front. Conversely, the collapse and clastic flow deposits are located farther away from the delta front, primarily distributed along the depression slope and slope angle. Finally, the turbidity flow deposits are the furthest from the delta front, predominantly found in the sheet-shaped deep lacustrine facies of the depression (Figure 13).

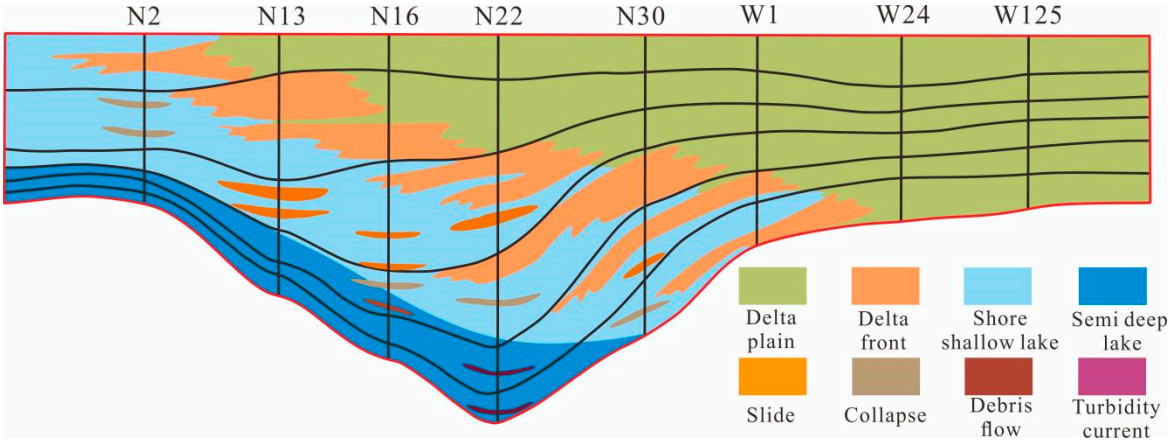

Figure 12. Profile distribution characteristics of delta and gravity flow sedimentary system in the Niuzhuang Sag.

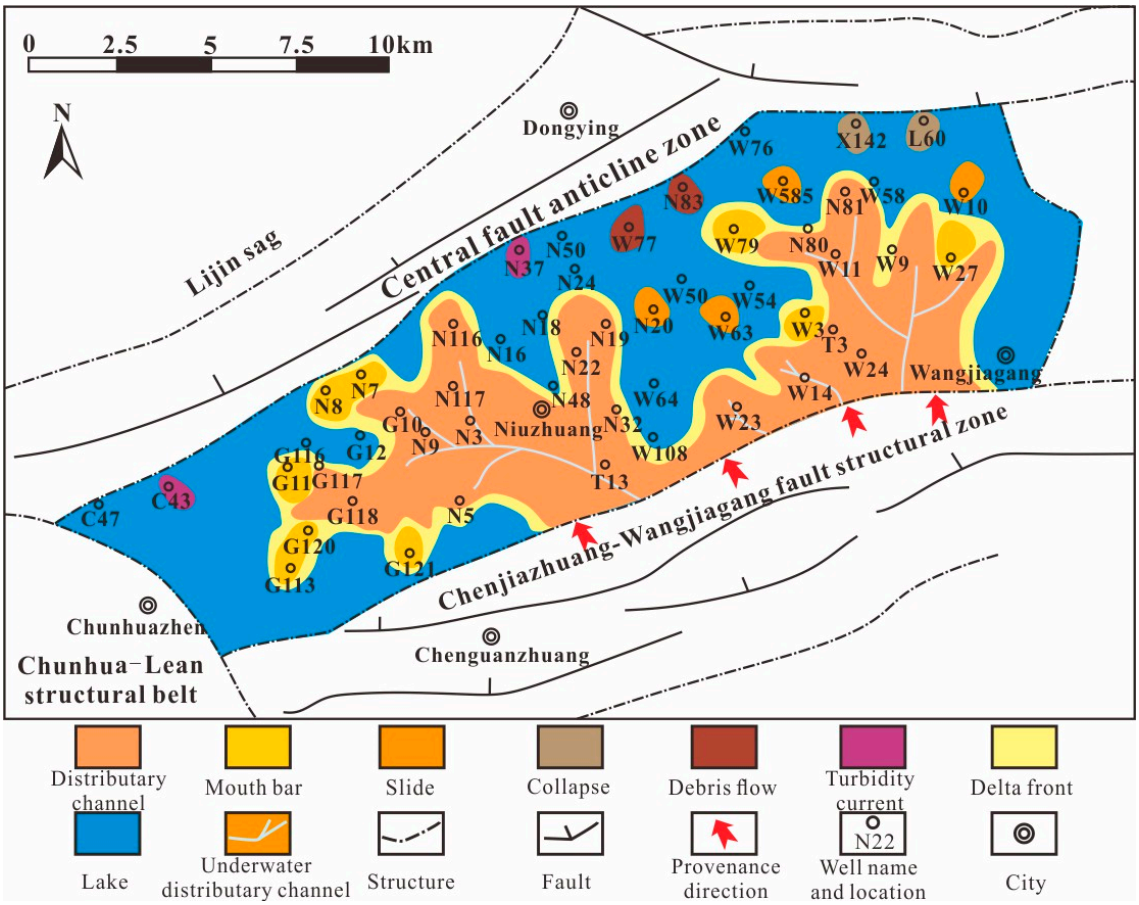

Figure 13. Plane distribution characteristics of delta and gravity flow sedimentary system in the Niuzhuang Sag.

5.3. Sedimentary Model

The Niuzhuang Sag delta is primarily situated in the southeast gentle slope zone, controlled by the Chenguanzhuang–Wangjiagang fault structural belt. During the deposition of the third member of the Shahejie Formation, multiple sedimentary processes led to the accumulation of underwater distributary channels and estuarine bar sand bodies on the southeastern slope of the depression. The delta front sand bodies experience slippage and collapse through geological evolution, subsequently being transported along the frontal slope toward the depression, forming a series of gravity flow sand bodies originating from different sources. These gravity flow sand bodies can be classified into four types: sliding deposits, collapse deposits, clastic flow deposits, and turbidite flow deposits. The sliding deposits are mainly distributed in the outer region of the delta front sand body. Under the influence of gravity, external tectonic forces, storms, and seasonal flooding, the sediment continues to move deeper down the slope. Some sediment deposits undergo deformation, rotation, and accumulation on the slope, forming collapse deposits, while others form clastic flow deposits. The finest-grained sediments eventually settle and become suspended deep within the depression, forming matted turbidite flow deposits (Figure 14).

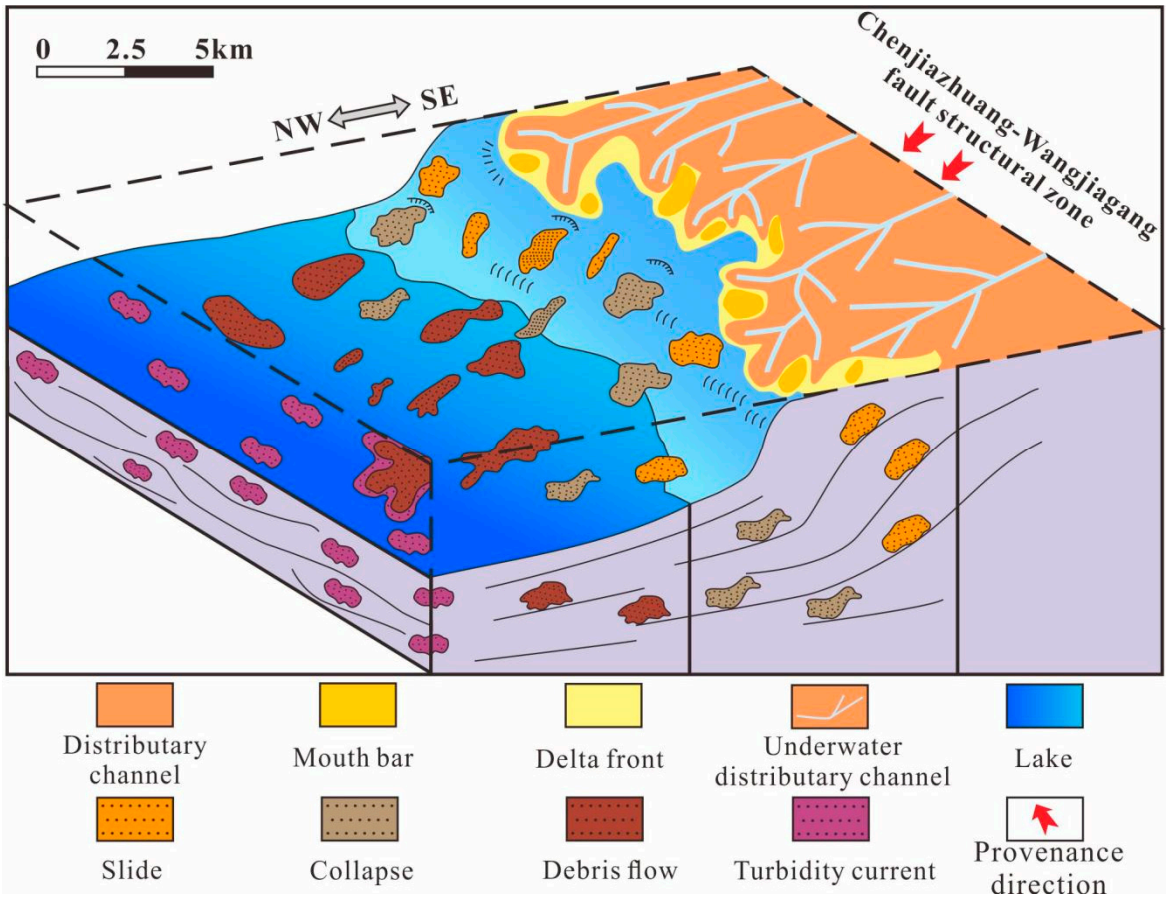

Figure 14. The sedimentary modes of the delta and gravity flow system in the Niuzhuang Sag.

6. Conclusions

The delta sand bodies of the third member of the Shahejie Formation in the Niuzhuang Sag predominantly belong to the delta front subfacies. The primary types of sand bodies are subaqueous distributary channels and estuarine bar sand bodies. Additionally, there are four types of gravity flow sand bodies: sliding deposits, collapse deposits, clastic flow deposits (sandy debris flow and muddy debris flow), and turbidite flow deposits.

The shale content of sliding, collapse, and muddy debris flow sedimentation is high, making it difficult to become an effective reservoir. Gravity flow sandstone reservoirs are

mainly formed with sandy debris flow and turbidity flow sedimentation. Among them, the pure block sandstone facies formed by sandy debris flow and the thick to extremely thick gravity flow sandstone composed of stacked block sandstones rich in mud and gravel have good sorting performance, fewer mudstone interlayers, and the best reservoir quality. Sandstone caused by turbidity flow has a low thickness and is often interbedded or interbedded with mudstone, resulting in poor reservoir quality.

During the deposition of the third member of the Shahejie Formation, the main body of the delta in the Niuzhuang Sag continuously accumulated within the depression, leading to the continuous buildup of underwater distributary channels and estuarine bar sand bodies on the southeastern slope of the depression. The sliding deposits are distributed in the outer part of the delta front sand body. Collapse deposits and clastic flow deposits are found on the slope and slope corner of the depression. The finest-grained sediments form matted turbidite flow deposits, which are distributed deep within the sag.

Author Contributions: Validation, K.G. and X.H.; resources, H.Z.; data curation, C.L.; writing—original draft preparation, Y.Z.; project administration, J.X. All authors have read and agreed to the published version of the manuscript.

Funding: This work was supported by the Natural Science Foundation of Shandong Province (No. ZR2022MD033).

Data Availability Statement: The data supporting the research results can be obtained from China Petrochemical Corporation Shengli Oil Field, but the availability of these data is limited. These data are used under the permission of the current research, so they are not disclosed. However, the author can provide data according to reasonable requirements and with the permission of China Petrochemical Corporation Shengli Oil Field.

Acknowledgments: Thank Shandong University of Science and Technology and Shengli Oil Field for their support to the project. The authors are also grateful to all who took part in the study. All authors have read and agreed to the published version of the manuscript.

Conflicts of Interest: The authors declare no conflict of interest.

References

1. Shanmegam, G. New perspectives on deep-water sandstones: Implications. *Pet. Explor. Dev.* **2013**, *40*, 294–301. [CrossRef]
2. Talling, P.J.; Allin, J.; Armitage, D.A.; Arnott, R.W.C.; Cartigny, M.J.B.; Clare, M.A.; Felletti, F.; Covault, J.A.; Girardclos, S.; Hansen, E.; et al. Key future directions for research on turbidity currents and their deposits. *J. Sediment. Res.* **2015**, *85*, 153–169. [CrossRef]
3. Pohl, F.; Eggenhuisen, J.T.; Tilston, M.; Cartigny, M.J.B. New flow relaxation mechanism explains scour fields at the end of submarine channels. *Nat. Commun.* **2019**, *10*, 4425. [CrossRef] [PubMed]
4. Feng, Z.Q.; Zhang, S.; Xie, X.N.; An, G.Z.; Zhao, B.; Hou, Y.P. Discovery of a Large-Scale Lacustrine Subaqueous Channel in the Nenjiang Formation of the Songliao Basin and Its Implication on Petroleum Geology. *Acta Geol. Sin.* **2006**, *80*, 1226–1232+1240.
5. Zou, C.N.; Zhao, Z.Z.; Yang, H.; Fu, J.H.; Zhu, R.K.; Yuan, X.J.; Wang, L. Genetic mechanism and distribution of sandy debris flows in terrestrial lacustrine basin. *Acta Sedimentol. Sin.* **2009**, *27*, 1065–1075.
6. Xian, B.Z.; Wang, J.H.; Liu, J.P.; Yin, Y.; Chao, C.Z. Classification and sedimentary characteristics of lacustrine hyperpycnal channels: Triassic outcrops in the south Ordos Basin, central China. *Sediment. Geol.* **2018**, *368*, 68–82. [CrossRef]
7. Cao, Y.C.; Jin, J.H.; Liu, H.N.; Yang, T.; Liu, K.Y.; Wang, Y.Z.; Wang, J.; Liang, C. Deep-water gravity flow deposits in a lacustrine rift basin and their oil and gas geological significance in eastern China. *Pet. Explor. Dev.* **2021**, *48*, 247–257. [CrossRef]
8. Guo, J.X.; Jiang, Z.X.; Xie, X.Y.; Liang, C.; Wang, W.W.; Busbey, A.B.; Jia, C.C.; Meng, J.Y. Deep-lacustrine sediment gravity flow channel-lobe complexes on a stepped slope: An example from the Chengbei Low Uplift, Bohai Bay Basin, East China. *Mar. Pet. Geol.* **2021**, *124*, 104839.
9. Li, W.H.; Zhou, L.F.; Fu, J.H.; Zhao, W.Z.; Xue, L.Q.; Jin, J.Q. Turbidity current deposits and their significance for petroleum geology of Upper Triassic in the Kuqa Depression. *Acta Sedimentol. Sin.* **1997**, *15*, 20–24.
10. Talling, P.J.; Masson, D.G.; Sumner, E.J.; Malgesini, G. Subaqueous sediment density flows: Depositional processes and deposit types. *Sedimentol. J. Int. Assoc. Sedimentol.* **2012**, *59*, 1937–2003.
11. Marchand, A.; Apps, G.; Li, W.; Rotzien, J.R. Depositional processes and impact on reservoir quality in deepwater paleogene reservoirs, us gulf of mexicoreservoir quality in deep water gulf of mexico paleogene trend. *AAPG Bull.* **2015**, *99*, 1635–1648. [CrossRef]
12. Zou, C.N.; Wang, L.; Li, Y.; Tao, S.Z.; Hou, L.H. Deep-lacustrine transformation of sandy debrites into turbidites, upper Triassic, central China. *Sediment. Geol.* **2012**, *265–266*, 143–155. [CrossRef]

13. Yang, T.; Cao, Y.C.; Wang, Y.Z.; Zhang, S.M. Types, sedimentary characteristics and genetic mechanisms of deep-water gravity flows: A case study of the middle submember in Member 3 of Shahejie Formation in Jiyang Depression. *Acta Pet. Sin.* **2015**, *36*, 1048–1059.
14. Xian, B.Z.; Wang, L.; Liu, J.P.; Lu, Z.Y.; Li, Y.Z.; Niu, S.W.; Zhu, Y.F.; Hong, F.H. Sedimentary characteristics and model of delta-fed turbidites in Eocene eastern Dongying Depression. *J. China Univ. Pet. (Ed. Nat. Sci.)* **2016**, *40*, 10–21.
15. Yao, Z.; Zhu, J.T.; Zuo, Q.M.; Man, X.; Mao, X.L.; Wang, Z.Z.; Dang, Y.Y. Gravity flow sedimentary system and petroleum exploration prospect of deep water area in the Qiongdongnan Basin. South China Sea. *Nat. Gas Ind.* **2015**, *35*, 21–30.
16. Li, S.L.; Yu, X.H.; Jin, J.L. Sedimentary Microfacies and Porosity Modeling of Deep-Water Sandy Debris Flows by Combining Sedimentary Patterns with Seismic Data: An Example from Unit I of Gas Field A, South China Sea. *Acta Geol. Sin. (Engl. Ed.)* **2016**, *90*, 182–194.
17. Yang, T.; Cao, Y.C.; Friis, H.; Liu, K.Y.; Wang, Y.Z.; Zhou, L.L.; Zhang, S.M.; Zhang, H.N. Genesis and distribution pattern of carbonate cements in lacustrine deepwater gravity-flow sandstone reservoirs in the third member of the Shahejie Formation in the Dongying Sag, Jiyang Depression, Eastern China. *Mar. Pet. Geol.* **2018**, *92*, 547–564. [CrossRef]
18. Haughton, P.; Davis, C.; Mccaffrey, W.; Barker, S. Hybrid sediment gravity flow deposits–classification, origin and significance. *Mar. Pet. Geol.* **2009**, *26*, 1900–1918. [CrossRef]
19. Talling, P.J.; Paull, C.K.; Piper, D. How are subaqueous sediment density flows triggered, what is their internal structure and how does it evolve? direct observations from monitoring of active flows. *Earth-Sci. Rev.* **2013**, *125*, 244–287. [CrossRef]
20. Stow, D.; Johansson, M. Deep-water massive sands: Nature, origin and hydrocarbon implications. *Mar. Pet. Geol.* **2000**, *17*, 145–174. [CrossRef]
21. Li, Y.F.; Pu, R.H.; Zhang, G.C.; Du, J.M.; Bao, J.J. New-type pliocene channel depositional systems resulting from turbidity flows obliquely interacting with contour currents: A novel case study from the southern Qiongdongnan basin, northern South China Sea. *Mar. Pet. Geol.* **2023**, *147*, 105982.
22. Shanmugam, G. 50 years of the turbidite paradigm (1950s–1990s): Deep-water processes and facies model—A critical perspective. *Mar. Pet. Geol.* **2000**, *17*, 285–342.
23. Du, C. Deposition pattern of stony and muddy debris flow at the confluence area. *J. Mt. Sci.* **2021**, *18*, 622–634. [CrossRef]
24. Zhou, X.P.; He, Q.; Liu, J.Y.; Li, S.X.; Yang, T. Features and origin of deep-water debris flow deposits in the Triassic Chang 7 Member, Ordos Basin. *Oil Gas Geol.* **2021**, *42*, 15.
25. Liu, X.J.; Liu, H.M.; Song, G.Q.; Jia, G.H.; Yang, H.Y. Sedimentary characteristics and distribution pattern of the slope-shifting fan in the low-lying slope zone of Dongying sag. *Pet. Geol. Recovery Effic.* **2016**, *23*, 1–10.
26. Zhang, H.A.; Wang, C.Z.; Jiang, F.H.; Jin, Y.Q.; Hu, B. Gravity flow deposits associating with ichnoassemblages within the middle Member 3 of Paleogene Shahejie Formation in Dongpu sag, Henan Province. *J. Palaeogeogr. (Chin. Ed.)* **2020**, *22*, 1157–1170.
27. Zhang, J.Q.; Li, S.X.; Li, H.W.; Zhou, X.P.; Liu, J.Y.; Guo, R.L.; Chen, J.L.; Li, S.T. Gravity flow deposits in the distal lacustrine basin of the 7th reservoir group of Yanchang Formation and deepwater oil and gas exploration in Ordos Basin: A case study of Chang 7_3 sublayer of Chengye horizontal well region. *Acta Pet. Sin.* **2021**, *42*, 570–587.
28. Shi, J.C.; Qu, X.F.; Lei, Q.H.; Qi, Y.; Li, S.H.; Xie, Q.C. Sedimentary characteristics and sand architecture of gravity flows in terrestrial lacustrine basins: A case study of Chang 7 Formation of the Upper Triassic in Ordos basin. *Geol. Exploration.* **2018**, *54*, 183–192.
29. Chen, B.Y.; Lin, C.Y.; Ma, C.F.; Ren, L.H.; Wang, J.; Li, Z.P.; Du, K. Types, characteristics and sedimentary model of deep-water gravity flow deposition in the steep slope zone of terrestrial faulted lacustrine basin: A case study of the Es4s submember in the Shengtuo area of Dongying depression. *Acta Geol. Sin.* **2019**, *93*, 2921–2934.
30. Huang, L.; Liu, C.Y. Evolutionary characteristics of the sags to the east of Tan–Lu Fault Zone, Bohai Bay Basin (China): Implications for hydrocarbon exploration and regional tectonic evolution. *J. Asian Earth Sci.* **2014**, *79*, 275–287.
31. Wang, W.Q.; Liu, N.; Tian, F. Sequence Stratigraphic Analysis of the Member 3 of Shahejie Formation in the Niuzhuang Area of the Dongying Depression. *J. Stratigr.* **2007**, *31*, 567–572.
32. Zhu, X.M.; Dong, Y.L.; Yang, J.S.; Zhang, Q.; Li, D.J.; Xu, C.G.; Yu, S. The sequence framework and depositional system distribution of Paleogene in Liaodong Bay area. *Sci. China Ser. D Earth Sci.* **2008**, *38* (Suppl. S1), 1–10. [CrossRef]
33. Shanmugam, G. *New Perspectives on Deep-Water Sandstones, Volume 9: Handbook of Petroleum Exploration and Production*; Elsevier: Amsterdam, The Netherlands, 2012; Volume 9, pp. 1–542.
34. Pickering, K.T.; Hiscott, R.N.; Hein, F.J. *Deep Marine Environments: Clastic Sedimentation and Tectonics*; Unwin Hyman: London, UK, 1989; p. 416.
35. Hampton, M.A. The role of subaqueous debris flow in generating turbidity currents. *J. Sediment. Petrol.* **1972**, *42*, 775–793.
36. Middleton, G.V.; Hampton, M.A. *Sediment Gravity Flows: Mechanics of Flow and Deposition*; Pacific Section Society of Economic Paleontologists and Mineralogists: Los Angeles, CA, USA, 1973; pp. 1–38.
37. Lowe, D.R. Sediment gravity flows: II. Depositional models with special reference to the deposits of high-density turbidity currents. *J. Sediment. Petrol.* **1982**, *52*, 279–297.
38. Kuenen, P.H. Properties of turbidity currents of high density. *Spec. Publ.* **1951**, *2*, 14–33.
39. Serra, O. *Fundamentals of Well-Log Interpretation: The Acquisition of Logging Data*; Elsevier: New York, NY, USA, 1984; pp. 1–423.

40. Zeng, H.L.; Backus, M.M.; Barrow, K.T. Stratal slicing, PartI: Realistic 3-D seismic model. *Geophysics* **1998**, *63*, 502–513. [CrossRef]
41. Zeng, H.L.; Henry, S.C.; Riola, J.P. Stratal slicing. Part II: Real 3-D seismic data. *Geophysics* **1998**, *63*, 514–522. [CrossRef]

Disclaimer/Publisher's Note: The statements, opinions and data contained in all publications are solely those of the individual author(s) and contributor(s) and not of MDPI and/or the editor(s). MDPI and/or the editor(s) disclaim responsibility for any injury to people or property resulting from any ideas, methods, instructions or products referred to in the content.